Tissue Examination to Monitor Antiangiogenic Therapy: A Phase I Clinical Trial with Endostatin[1]

Christoph Mundhenke, James P. Thomas, George Wilding, Fred T. Lee, Fred Kelzc, Rick Chappell, Rosemary Neider, Linda A. Sebree, and Andreas Friedl[2]

Comprehensive Cancer Center [C. M., J. P. T., G. W., F. T. L., F. K., R. C., R. N., A. F.], Department of Pathology and Laboratory Medicine [L. A. S., A. F.], and Department of Biostatistics [R. C.], University of Wisconsin Madison, Wisconsin 53792; and Department of Obstetrics and Gynecology, University of Kiel, 24105 Germany [C. M.]

ABSTRACT

***Purpose*: The purpose of this study was to determine the effect of the angiogenesis inhibitor endostatin on blood vessels in tumors and wound sites.**

***Experimental Design*: In a Phase I dose escalation study, cancer patients were treated with daily infusions of human recombinant endostatin. Tumor biopsies were obtained prior to and 8 weeks after initiation of treatment. Blood vessel formation in nonneoplastic tissue was evaluated by creating a skin wound site on the arm with a punch biopsy device. The wound site was sampled with a second biopsy after a 7-day interval. This sequential biopsy procedure was performed prior to and 3 weeks after initiation of endostatin treatment. Vascular density, endothelial cell kinetics, and blood vessel maturity were determined in tumor and skin wound samples. The ultrastructure of tumor blood vessels was examined by electron microscopy.**

***Results*: As expected, the tumors were of variable vascular density. Skin wounding induced a vascular granulation tissue containing a high percentage of proliferating endothelial cells. The proportion of immature blood vessels was high in tumors and in wound sites and low in normal skin. No statistically significant difference was detected between pretreatment and treatment samples of tumors and of skin wounds for any of the parameters tested.**

***Conclusions*: Endostatin treatment was not associated with any recognizable vascular changes in tumor samples and did not perturb wound healing at the doses and the treatment schedule used.**

Received 3/1/01; revised 7/2/01; accepted 7/31/01.

The costs of publication of this article were defrayed in part by the payment of page charges. This article must therefore be hereby marked *advertisement* in accordance with 18 U.S.C. Section 1734 solely to indicate this fact.

[1] This study was supported by NIH Grant UO1 CA62491.

[2] To whom requests for reprints should be addressed, at University of Wisconsin, Department of Pathology, Clinical Sciences Center K4/850, 600 Highland Avenue, Madison, WI 53792. Phone: (608) 265-9283; Fax: (608) 265-6215; E-mail: afriedl@facstaff.wisc.edu.

INTRODUCTION

Neoplasms depend on the formation of new of blood vessels (angiogenesis) for continued growth and metastatic spread. Without angiogenesis, tumors remain small and do not threaten the life of the host (1). In normal resting tissues, where blood vessel growth is minimal, angiogenesis is controlled by a balance of angiogenic stimulators and inhibitors. This balance is perturbed in tumors to favor angiogenesis either by overproduction of angiogenesis inducers or by lack of inhibitors (2).

Recently, several naturally occurring angiogenesis inhibitors have been identified. The most potent inhibitor appears to be endostatin, the COOH-terminal proteolytic fragment of the basement membrane component collagen XVIII (3). In a xenotransplantation model, endostatin administration leads to pronounced tumor regression, suggesting that the peptide induces regression of existing blood vessels in addition to preventing the growth of new ones (3, 4). Preclinical experiments targeting endogenous tumors have shown less dramatic results. The mechanism of action of endostatin is unclear. It inhibits endothelial cell proliferation *in vitro* (5, 6). Different investigators have proposed interference with vascular endothelial cell growth factor and fibroblast growth factor-2 (basic fibroblast growth factor) pathways (7), induction of endothelial cell apoptosis (8, 9), and inhibition of matrix metalloproteases (10). Inhibition of endothelial cell migration by modulating c-*myc* levels has also be proposed (11). Endostatin possesses a prominent heparan sulfate binding domain (12), but at present it is unresolved whether this domain is required for antiangiogenic activity (6, 13, 14). We have described the ability of endostatin to interact with vascular basement membranes independent of its heparan sulfate binding domain (15).

Recent successes in producing active human recombinant endostatin in yeast in large quantities have allowed testing of this protein in early clinical studies (16, 17). Antiangiogenic treatment strategies offer a number of compelling advantages over conventional cytotoxic cancer therapies that have been highlighted in recent reviews (18). Briefly, endothelial cells, the drug targets, are readily accessible to pharmacological agents. The ratio of tumor cells to endothelial cells has been estimated as 100:1 (1), leading to the expectation of an amplified antitumor effect when endothelial cells are successfully inhibited. Probably most importantly, in contrast to genetically unstable tumor cells, endothelial cells are genetically stable, making it unlikely that antiangiogenic agents would induce drug resistance (19). This latter argument is powerfully supported by preclinical studies (4).

Designing clinical trials with angiogenesis inhibitors is hampered by the fact that it is very difficult to determine the optimal dose and administration regimen. Treatment with cytotoxic drugs has typically been optimized by determining the

MTD.[3] Pure antiangiogenic agents would be expected to have a low toxicity, and the MTD may be far higher than the biologically optimal dose. In addition, administration of the MTD of a biological inhibitor such as endostatin may not be economically feasible. Ideally, antiangiogenic therapy should be titrated based on biological end points. There are no established assays for measuring angiogenesis (or its inhibition) in humans. In animal models, corneal angiogenesis assays are the gold standard, but skin angiogenesis assays have also been used successfully (20). A skin wounding assay has also recently been described in humans (21, 22). Blood vessel formation in healing wounds as a surrogate angiogenesis assay may not exactly mirror tumor angiogenesis, but it may provide important information on antiangiogenic activity and predict delayed wound healing as a potential adverse effect of angiogenesis inhibitors.

Here we report on the results of blood vessel examination in tissues of wound sites and tumors in patients of an NCI-sponsored Phase I dose escalation trial with the angiogenesis inhibitor endostatin at the University of Wisconsin Comprehensive Cancer Center. Blood vessels were characterized quantitatively and qualitatively by determining vascularity, endothelial cell kinetics, and blood vessel maturity. Comprehensive analysis of blood vessels *in situ* may serve as a model for future trials with antiangiogenic agents and help define surrogate end points for such studies.

MATERIALS AND METHODS

Patients and Treatment. Twenty-one cancer patients with nonhematological malignancies without brain metastases who had progressed on standard therapies were recruited for a Phase I dose escalation study testing the tolerability of the angiogenesis inhibitor endostatin. Human recombinant endostatin produced in yeast (Entremed, Rockville, MD) was administered by daily infusions at six dose levels (30–300 mg/m^2) until progression. Informed consent and Institutional Review Board approval were obtained for all procedures.

Skin Biopsies. Two sequential skin biopsies were performed with a 4-mm punch biopsy device (Accuderm) in the same location on the upper arm, to assess blood vessel formation in wound sites. The purpose of the first biopsy was to create a wound, whereas the second biopsy 7 days later captured the wound tissue. Such sequential biopsy pairs were collected prior to and 3 weeks into endostatin treatment (see Fig. 1). The skin punch biopsy cylinders were fixed in 10% buffered formalin and routinely embedded in paraffin.

Tumor Biopsies. Tumor tissue was sampled prior to and 8 weeks into endostatin treatment (Fig. 1). The samples were obtained with a 18-gauge true-cut needle core biopsy device under ultrasound or computed tomography guidance. The tissue cores were submitted fresh to the surgical pathology laboratory,

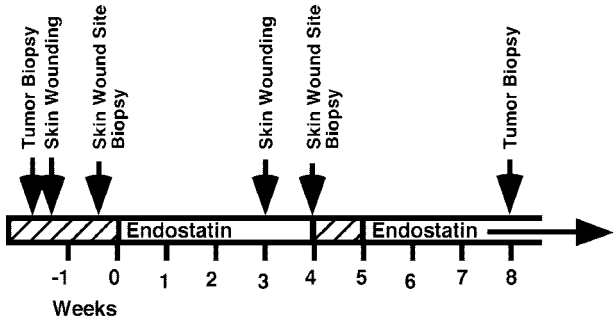

Fig. 1 Time schedule for biopsies relative to treatment. Two pairs of skin biopsies were taken: one prior to initiation of endostatin therapy, and one 3 weeks after the beginning of treatment. Tumor biopsies were obtained before and 8 weeks into endostatin treatment. Treatment was interrupted during the 5th week and then reinstituted beyond 8 weeks until tumor progression.

and one half was fixed in 10% buffered formalin and routinely embedded in paraffin. The other half was divided into a small sample for electron microscopy, and the rest was embedded in OCT compound and snap-frozen to −70°C.

Immunohistochemical Labeling. Four-μm-thick paraffin sections on "Plus" slides were baked, deparaffinized, and rehydrated. Heat-induced epitope retrieval was performed on all slides by immersion of the slides in 1 mM EDTA (pH 8) and incubation in an electric pressure cooker (BioCare Medical, Walnut Creek, CA) for 3 min at 25 psi. The slides were placed on the ES automated immunohistochemical stainer (Ventana Medical Systems, Tucson, AZ).

Ki67 labeling was performed using a monoclonal antibody (clone 7B11; Zymed Laboratories, San Francisco, CA) at a 1:75 dilution for 28 min at 42°C, followed by an amplification kit and the diaminobenzidine basic detection system (both Ventana Medical Systems). Labeling for MSA required pretreatment with protease 3 (Ventana). Anti-MSA mouse monoclonal antibody (clone HHF35; BioCare) was applied as a prediluted preparation for 20 min at 42°C, followed by the diaminobenzidine detection system. Labeling for either of these antigens was followed by staining with the endothelial marker CD31. Incubation with the anti-CD31 antibody (clone JC/70A, prediluted; NeoMarkers, Freemont, CA) for 4 min was followed by reaction with the amplified alkaline phosphatase Fast Red detection system (Ventana).

A pale Harris hematoxylin counterstain was the final step in the automated procedure. At completion, the slides were removed from the stainer, rinsed free of coverslip oil, dehydrated through graded alcohols, and cleared in xylene. Slides were coverslipped with a synthetic mounting medium. The technician was blinded to the subjects' treatment status and dose levels.

Analysis of Blood Vessel Density. Three images were acquired from each CD31/Ki67 dual-labeled tissue section by brightfield microscopy (Olympus BX40, ×20 objective) and a digital camera (SV Micro). The CD31-positive area (A_{CD31}) and total area covered by tissue (A_t) were measured using the "magic wand" tool within the Photoshop program (Adobe). The CD31-LI was defined as A_{CD31}/A_t and expressed as a percentage.

[3] The abbreviations used are: MTD, maximal tolerated dose; MSA, muscle-specific actin; CD31-LI, CD31 labeling index; pEC-LI, proliferating endothelial cell labeling index; VII, vascular immaturity index; TUNEL, terminal deoxynucleotidyl transferase (Tdt)-mediated nick end labeling; vWF, von Willebrand factor; MVD, microvessel density; TSP-1, thrombospondin-1.

Analysis of Endothelial Cell Proliferation. Proliferating endothelial cells were identified as cells showing both nuclear staining for Ki67 and cytoplasmic staining for CD31. The area of Ki67-positive endothelial cell nuclei was determined by manually selecting each nucleus with the magic wand tool within Photoshop. The pEC-LI was defined as the ratio of the Ki67-positive nuclear area in (CD31-positive) endothelial cells (A_{Ki67EC}) and the CD31-positive area (A_{Ki67EC}/A_{CD31}).

Analysis of Blood Vessel Maturity. The proportion of immature blood vessels was determined by a dual-label procedure for MSA and CD31 (see above). Staining resulted in a red signal for CD31 and a brown signal for MSA. Blood vessels invested by MSA-positive cells and blood vessels devoid of actin-positive support cells were counted manually using a grid ocular at ×100 magnification. CD31-positive structures without a vascular lumen, arteries, or veins were not counted. The VII was calculated by dividing the number of MSA-negative vessels by the total number (MSA positive or negative) blood vessels.

Analysis of Endothelial Cell Apoptosis. Endothelial cell apoptosis was detected by dual labeling of tissues with the TUNEL procedure and with anti-vWF antibodies. Four-μm sections of paraffin-embedded tissues were rehydrated and treated with sodium borohydride (13.2 mM) for 15 min and glycine (0.1 M) overnight to reduce autofluorescence. Apoptotic cells were identified using the *In Situ* Cell Death Detection, POD kit (Roche-Boehringer Mannheim, Indianapolis, IN), according to the manufacturer's instructions but omitting the signal conversion reaction. During the labeling reaction, the terminal deoxynucleotidyl transferase adds fluorescein-tagged nucleotides at sites of double-stranded and single-stranded DNA breaks. Endothelial cells were identified with anti-vWF antibody (Neomarkers) at a dilution of 1:60 and visualized with an Alexa546-conjugated secondary antibody. Slides were viewed with a Nikon microscope equipped for epifluorescence and fitted with a chilled charge-coupled device camera (Photometrics, Roper Scientific, Trenton, NJ). Images were acquired in the "green" emission channel to detect TUNEL-positive cells and the "red" emission channel to detect blood vessels. Apoptotic endothelial cells were defined as both TUNEL positive and vWF positive.

Ultrastructural Analysis of Blood Vessels. For transmission electron microscopy, tissues were minced into 1-mm cubes and fixed in 2.5% glutaraldehyde in Sorensen's phosphate buffer (pH 7.4). Tissues were subsequently washed, postfixed in Caulfield's osmium tetroxide fixative for 2 h at 4°C, dehydrated through a series of graded ethanols and propylene oxide, embedded in Epon-Spurr resin, and polymerized overnight at 78°C. Thin sections were cut on a Reichert-Jung ultramicrotome and stained with saturated aqueous uranyl acetate and lead citrate. Grids were examined with a Hitachi H-600 transmission electron microscope at 75 kV.

Statistical Analysis. The microscopists (A. F. and C. M.) were blinded to the subjects' treatment status for all analyses. Means and confidence intervals were calculated using the logarithm of the crude measurements and subsequently exponentiated. Results were tested for statistical significance by the paired two-tailed Student's *t* test, also on the logarithmic scale. All calculations were done with Microsoft Excel software on an Apple Macintosh G3 computer.

Table 1 Diagnoses of patients admitted into the Phase I endostatin trial

The numbers in parentheses indicate the numbers of cases with complete biopsy pairs containing sufficient material for blood vessel analysis.

Colorectal carcinomas, $n = 6$ (3)
Sarcomas, $n = 4$ (2)
Lung carcinomas, $n = 3$ (0)
Stomach carcinoma, $n = 1$ (0)
Prostate carcinoma, $n = 1$ (0)
Kidney carcinoma (clear cell type), $n = 1$ (0)
Adrenocortical carcinoma, $n = 1$ (0)
Ovarian carcinoma, $n = 1$ (1)
Head and neck squamous cell carcinoma, $n = 1$ (1)
Malignant melanomas, $n = 2$ (1)

RESULTS

Patients and Tumor Biopsies. A total of 21 patients were recruited into the study, representing a wide spectrum of malignancies (Table 1). Tumor biopsies were performed on all 21 patients prior to initiation of endostatin treatment, and viable tumor tissue amenable to blood vessel analysis was present in 14 cases as initially assessed by H&E stains. Tumor progression and ensuing departure from the study during the first 8 weeks of treatment occurred in 10 patients and was the most common reason for lack of a second biopsy sample. Of the remaining 11 second tumor biopsy samples, 2 did not contain sufficient viable tumor tissue. Eight complete pairs of pretreatment and treatment tumor biopsies remained to assess treatment effect. The cases were distributed throughout the different dose levels (Table 1).

Tumor Samples. Sections of tumor tissue were analyzed simultaneously for presence and localization of the endothelial cell marker CD31 and the proliferation marker Ki67 (Fig. 2, *A* and *B*). Tumor vascularity was expressed as CD31-LI. As expected, tumors showed a wide spectrum of CD31-LI values ranging from 2 to 14%. The highest vascularity was observed in a renal cell carcinoma (Fig. 2*A*) and in a high-grade sarcoma (not shown). CD31 and pEC-LI values did not positively correlate, supporting the notion that vascular density is not necessarily related to angiogenic activity. Interestingly, endothelial cells in the highly vascular sarcoma displayed the lowest proliferative activity, whereas endothelial cells in a much less vascular squamous cell carcinoma of the head and neck region were highly proliferative (Fig. 2*B*).

Endostatin treatment did not result in a consistent or statistically significant CD31-LI change in the eight biopsy pairs available for comparison (Fig. 2*C*). This result does not exclude the possibility of angiogenesis inhibition in the tumor samples because a proportional reduction of endothelial cells and tumor cells would not be detectable with this analysis. Endothelial cell proliferation, expressed as pEC-LI also did not change significantly from pretreatment to treatment samples (Fig. 2*D*). Blood vessel growth would be expected to be a function of the balance of endothelial cell proliferation and death. Therefore, endothelial cell apoptosis was also measured in the tumor samples. Endothelial cell apoptosis was defined as colocalization of TUNEL signal and the endothelial cell marker vWF. Apoptotic endothelial cells were rarely identified in tumor sections (4 cells

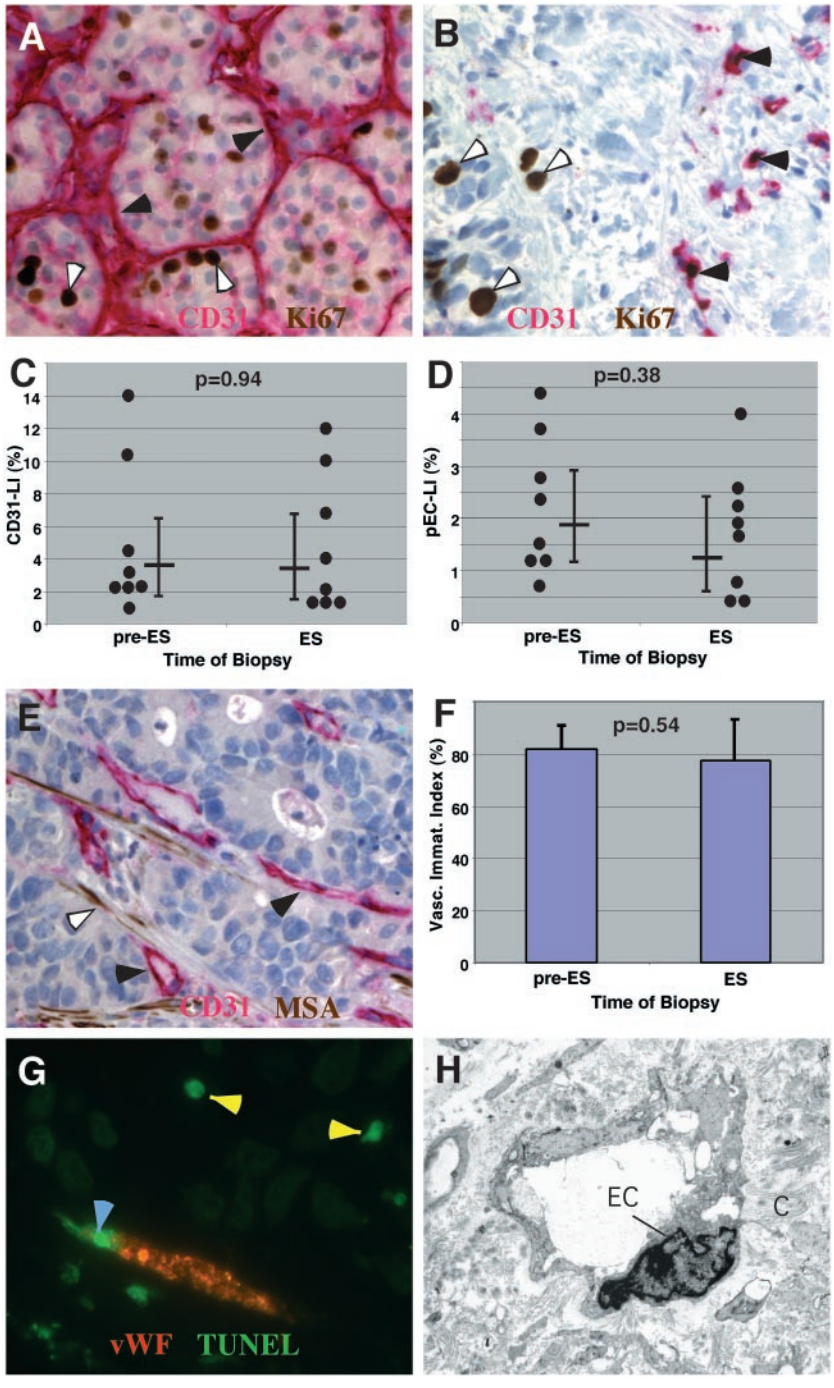

Fig. 2 Characterization of blood vessels in tumor biopsies. Samples of tumor tissue were obtained prior to and 8 weeks after initiation of endostatin treatment. Paraffin sections were analyzed with three dual-labeling reactions (*A*, *B*, *E*, and *G*) to assess vascular density, endothelial cell proliferation, blood vessel maturity, and endothelial cell death. *A*, section of a metastatic renal cell carcinoma. Dual labeling is shown for the endothelial marker CD31 (*magenta*) and proliferation marker Ki67 (*brown*). *Filled arrowheads* indicate the dense vascular network lacking proliferating endothelial cells; *open arrowheads* indicate proliferating tumor cells (magnification, ×400). *B*, section of a metastatic poorly differentiated squamous cell carcinoma from the head and neck region. Dual labeling for CD31 (*magenta*) and Ki67 (*brown*) is shown. *Filled arrowheads* indicate proliferating endothelial cells; *open arrowheads* indicate proliferating tumor cells (magnification, ×400). *C*, computer-assisted quantitative assessment of tumor vascularity: Vascular density is expressed as CD31-LI. ●, individual measurements. The *horizontal lines* indicate the geometric mean; the *vertical lines* indicate the 95% confidence interval. *D*, computer-assisted quantitative assessment of endothelial cell proliferation (*pEC-LI*). ●, individual measurements; The *horizontal lines* indicate the geometric mean; the *vertical lines* indicate the 95% confidence interval. *E*, section of metastatic colorectal carcinoma. Dual labeling for CD31 (*magenta*) and MSA as pericyte marker (*brown*) is shown. *Filled arrowheads* indicate immature blood vessels lacking pericytes; *open arrowhead* indicates MSA-positive stromal myofibroblasts (magnification, ×400). *F*, semiquantitative assessment of blood vessel maturity. Blood vessels sheathed by pericytes and blood vessels lacking pericytes were counted manually with a grid ocular. The results were expressed as VII (*Vasc. Immat. Index*), defined as the ratio of immature blood vessels lacking pericytes to the total number of blood vessels. The *columns* indicate means; the *bars* indicate 95% confidence intervals. *G*, section of high-grade sarcoma, Endothelial cell apoptosis was detected by dual labeling for endothelial cell marker vWF (*red*) and apoptosis by the TUNEL assay (*green*). Blood vessels contain only rare apoptotic cells (*yellow arrowhead*), whereas numerous tumor cells undergo apoptosis (*light blue arrowheads*; magnification, ×630). *H*, section of ovarian carcinoma, as shown by transmission electron microscopy. A capillary is lined by swollen endothelial cells (*EC*) and surrounded by fibrillar collagen (*C*). Magnification, ×5200. *ES*, endostatin.

in 18 tumor sections; Fig. 2*G*), whereas tumor cell apoptosis was a frequent event in some tumors (Fig. 2*G*), serving as internal positive control. Endostatin treatment did not increase the proportion of TUNEL-positive endothelial cells.

Newly formed blood vessels distinguish themselves initially from their mature counterparts by a lack of MSA-containing pericytes. Mature vessels are characterized in tissue sections by a central layer of CD31-positive endothelial cells and a peripheral rim of actin-positive pericytes (Fig. 3*E*). Immature vessels were defined as CD31 positive only. The proportion of immature blood vessels has been postulated to represent a measure of the angiogenic activity in a given tissue (23, 24). This ratio varied widely among tumors, but was not significantly different between pretreatment and treatment samples (Fig. 2*F*). In addition, examination of blood vessels by electron microscopy (Fig. 2*H*) revealed variations from tumor to tumor and from field to field, but no discernable treatment-associated alteration.

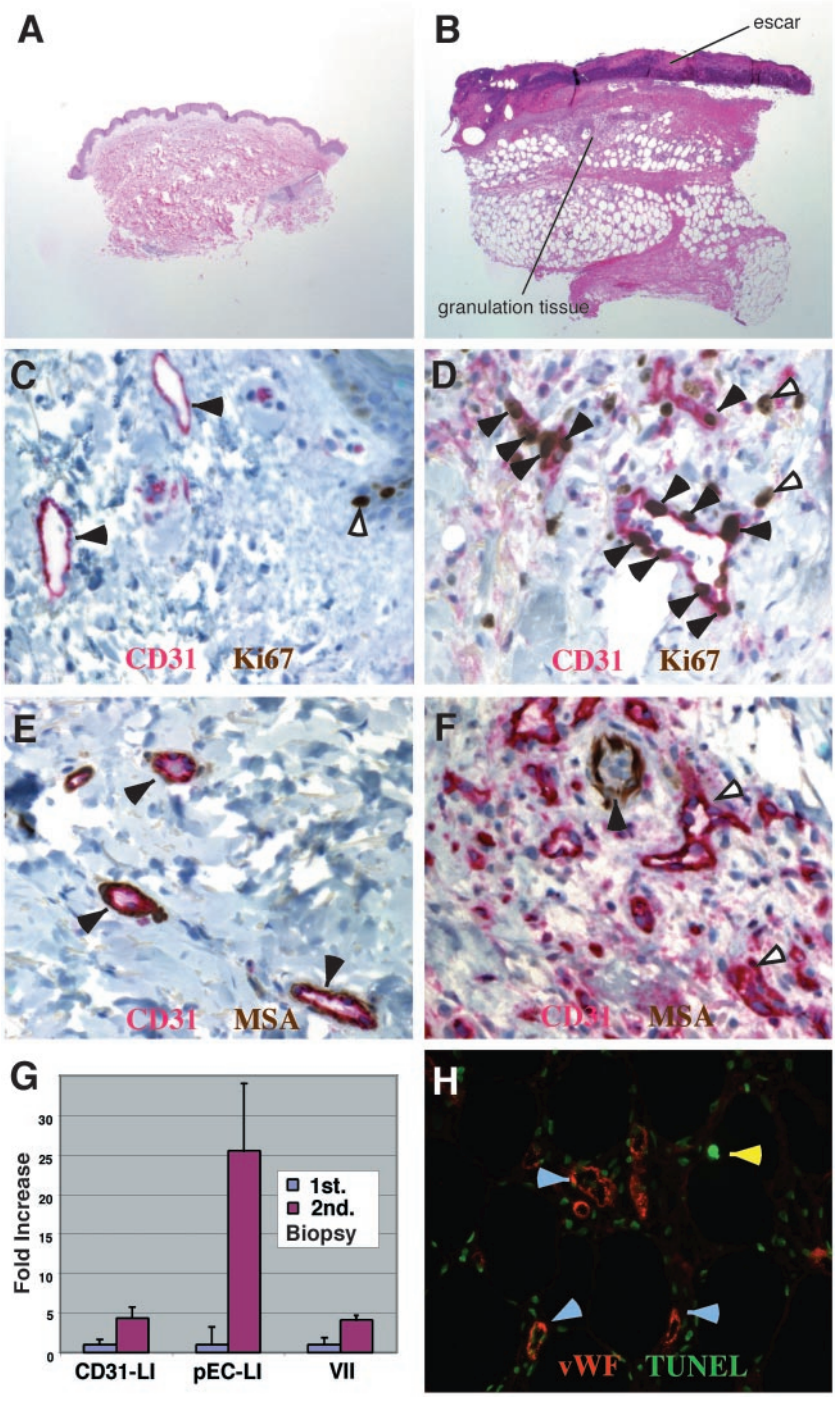

Fig. 3 Skin wounding assay to measure angiogenic activity *in vivo*. A 4-mm punch biopsy of skin was taken to generate a wound site. Seven days later, the wound site was biopsied. Paraffin sections of the normal skin tissue present in the first biopsy sample and of wound site tissue present in the second biopsy sample were stained with H&E (*A* and *B*) and analyzed with three dual-labeling reactions (*C–F* and *H*) to assess vascular density, endothelial cell proliferation, blood vessel maturity, and endothelial cell death. *A*, H&E-stained section of normal skin from first biopsy sample (magnification, ×20). *B*, H&E-stained section from second biopsy sample. Dermis and subcutis contain a florid granulation tissue, and the skin surface is covered by escar (magnification, ×20). *C*, section of normal skin, showing dual labeling for the endothelial marker CD31 (*magenta*) and the proliferation marker Ki67 (*brown*). *Filled arrowheads* indicate blood vessels with quiescent endothelial cells; *open arrowhead* indicates proliferating basal keratinocyte (magnification, ×400). *D*, section of wound site showing dual labeling for CD31 (*magenta*) and Ki67 (*brown*). *Filled arrowheads* indicate proliferating endothelial cells; *open arrowheads* indicate proliferating cells other than endothelial cells (magnification, ×400). *E*, section of normal skin showing dual labeling for CD31 (*magenta*) and MSA as pericyte marker (*brown*). *Filled arrowheads* indicate mature blood vessels sheathed by pericytes (magnification, ×400). *F*, section of wound site showing dual labeling for CD31 (*magenta*) and MSA (*brown*). *Open arrowheads* indicate immature blood vessels lacking pericyte sheathing; *filled arrowhead* indicates a sweat duct as an internal positive control (magnification, ×400). *G*, quantitative assessment of vascular density (*CD31-LI*), endothelial cell proliferation (*pEC-LI*), and blood vessel maturity (*VII*) in three pairs of first and second biopsies. Results are expressed as *Fold stimulation* relative to results of first biopsy; *bars*, 95% confidence intervals. Wounding induces active angiogenesis with an increase of all three parameters. *H*, section of wound site showing detection of endothelial cell apoptosis by dual labeling for endothelial cell marker vWF (*red*) and apoptosis by TUNEL assay (*green*). Blood vessels (*light blue arrowheads*) contain only very sparse apoptotic cells (not seen in this section), whereas occasional extravascular stromal cells (*yellow arrowhead*) and keratinocytes (not seen in this section) undergo apoptosis (magnification, ×200).

Wound Healing. Angiogenesis is an important component of wound healing. Therefore, we chose to observe wound healing in patients receiving endostatin. Typically, blood vessels begin to sprout and grow 4–7 days after injury and represent a major component of granulation tissue, in addition to (myo-) fibroblasts and inflammatory cells. Wound sites were generated in study patients with a routine punch biopsy procedure, and the wound granulation tissue was sampled 7 days later. Preliminary experiments in volunteers (not shown) led to the conclusion that florid blood vessel formation was present after that time interval.

Initially, we characterized blood vessels in normal skin and in wound sites. Punch biopsy cylinders of wound sites appeared expanded (Fig. 3*B*) compared with biopsy material from normal skin (Fig. 3*A*) because of edema and an increase in cellularity (inflammatory cells, myofibroblasts, and endothelial cells). As

expected, the vascularity (expressed as CD31-LI) in wound sites was vastly greater than in normal skin (Fig. 3, *C*, *D*, and *G*). The difference between normal skin and wound tissue was even more pronounced when endothelial cell proliferation was evaluated. Endothelial cells in normal skin were mostly Ki67 negative (Fig. 3*C*), whereas the proportion of Ki67-positive endothelial cells in skin wounds exceeded that of normal skin by a factor of 25 and of tumor vessels by a factor of >6 (Fig. 3, *D* and *G*). Similar to our findings in tumors, apoptosis was also a rare event in wound tissue. Of 11 skin wound sections examined, only two TUNEL-positive endothelial cells were identified (one in a pretreatment and one in a treatment sample; not shown). Scattered stromal cells and numerous keratinocytes at the wound edge were TUNEL positive, serving as internal positive control (Fig. 3*H*). The high level of proliferation and the low degree of apoptosis in skin wound endothelial cells provided an good baseline to assess potential effects of the angiogenesis inhibitor endostatin. As expected, the percentage of immature (MSA-negative) blood vessels was greatly increased in the granulation tissue (Fig. 3, *F* and *G*) compared with normal skin (Fig. 3, *E* and *G*).

Neither the extent of the granulation tissue core (Fig. 4*A*) nor vascularity (Fig. 4*B*) differed significantly between pretreatment and treatment samples. Mean endothelial cell proliferative activity was slightly reduced in samples from endostatin-treated patients, but this difference did not reach statistical significance ($P = 0.067$; Fig. 4*C*). No change in the proportion of immature blood vessels occurred during endostatin treatment (Fig. 4*D*). In addition, no apparent morphological differences between blood vessels in pretreatment and treatment samples were observed.

DISCUSSION

The goal of this study was to determine vascularization and angiogenic activity in patients receiving antiangiogenic therapy. Blood vessels were characterized comprehensively *in situ* by use of a combination of three dual-labeling reactions. This approach allowed us to measure vascular density, endothelial cell proliferation, endothelial cell death, and blood vessel maturity. The *in situ* assays were applied to both tumor specimens and tissue samples of experimental skin wounds. The purpose of the skin wounding experiment was to detect potential adverse effects of the antiangiogenic treatment on wound healing and to explore the possibility of using skin wounding as a surrogate assay for tumor angiogenesis. Tumors showed a heterogeneous distribution of vascular density, endothelial cell proliferation, and vascular maturity. Skin wounds were characterized by a high vascular density and actively proliferating endothelial cells. The proportion of immature blood vessels was similar in skin wounds and in tumors and was much higher than in normal skin. We were unable to detect any changes in blood vessels associated with endostatin treatment in this limited Phase I clinical trial. The main questions raised by these results are the following: (*a*) Are there differences between angiogenesis in tumors and healing wounds and is wound healing a valid surrogate end point for tumor angiogenesis? (*b*) What tissue-based assay(s) is/are best suited to determine angiogenic activity *in situ*? (*c*) Why do we fail to detect endostatin-induced changes in blood vessels?

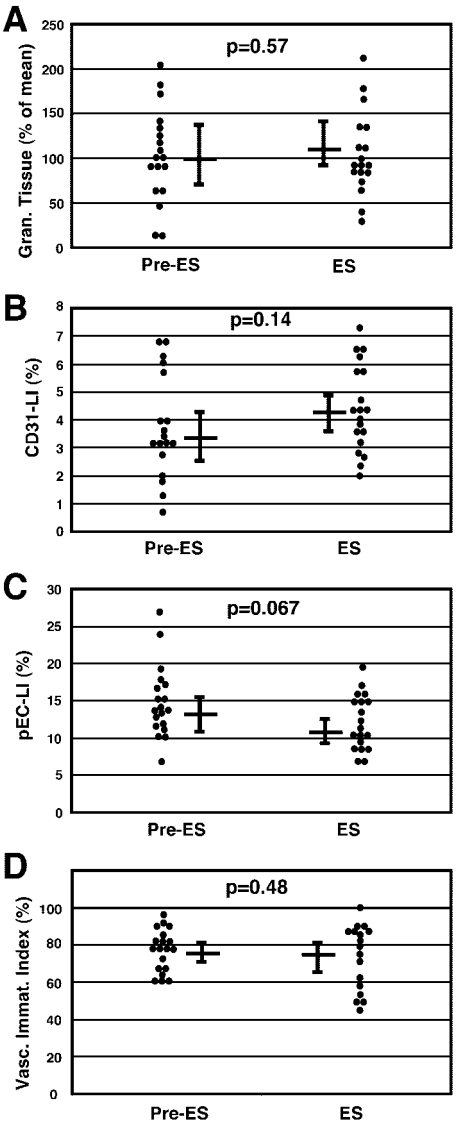

Fig. 4 Effect of endostatin treatment on skin wound sites. Quantitative and semiquantitative analysis of blood vessels in wound sites was performed before (*pre-ES*) and during (*ES*) endostatin therapy. *A*, semiquantitative measurement of granulation tissue size. The mean of the pretreatment samples was designated as 100%. *B*, quantitative assessment of vascular density, expressed as CD31-LI. ●, means of triplicates. *C*, quantitative measurement of endothelial cell labeling index (*pEC-LI*). ●, means of triplicates. *D*, semiquantitative assessment of blood vessel maturity: The percentage of blood vessels lacking pericytes is expressed as VII (*Vasc. Immat. Index*). ●, individual patients. The *horizontal bars* indicate geometric means; *vertical bars* indicate the 95% confidence intervals. *P* was determined by paired *t* test.

One issue brought up by this study relates to similarities and differences between tumor and wound angiogenesis and to the validity of using wounding as a surrogate end point for tumor angiogenesis. The stromal response to infiltrating cancer cells has been compared to "a wound that never heals" (25), and molecular approaches have identified many similarities between angiogenesis occurring in tumors and in benign processes. A

recent study identified complex but virtually identical gene expression patterns in the endothelium of a variety of tumors, healing wounds, and the corpus luteum (26). This uniformity is surprising, considering that the investigators used a technology (serial analysis of gene expression) that does not depend on preexisting databases of expressed genes and therefore provides an unbiased view of gene expression profiles.

It is, however, highly unlikely that angiogenesis occurring in wound granulation tissue will be an exact replica of tumor angiogenesis. The microenvironment in the wound site is clearly different, lacking tumor cells but being rich in inflammatory cells, platelets, and acellular constituents such as fibrinogen, fibrin, and other components of the clotting and fibrinolytic system. The question of whether agents such as endostatin selectively target tumor angiogenesis *versus* wound angiogenesis is subject to controversy. One group found no effect of endostatin treatment on wound healing in mice (27), whereas a different group of investigators detected subtle vascular changes in mice receiving endostatin (28). Mechanical wound strength rather than histological parameters were measured in the former study, whereas immunohistology and electron microscopy were used in the latter. Conflicting reports on the effects of angiogenesis inhibitors on wound healing are not limited to endostatin. Klein *et al.* (29) observed inhibition of murine skin wound healing by the fumagillin analogue TNP-470, whereas Tanaka *et al.* (30) saw no such effect. Again, the latter study was restricted to macroscopic and mechanical measurements, suggesting that more sensitive techniques may be required to detect wound angiogenesis inhibition.

We observed greatly (at least 6-fold) increased proliferative activity in wound site endothelial cells compared with tumor endothelial cells. Therefore, differences between tumor angiogenesis and wound angiogenesis may be largely quantitative in nature. One could argue that in wound sites, the balance of angiogenic stimulators and inhibitors is tilted far in favor of the stimulators, making it difficult for antiangiogenic drugs to overcome this angiogenic activity. Interestingly, however, antiangiogenic treatment appears to be most effective in situations of rapid blood vessel growth (24), *e.g.,* after implantation of angiogenic factors into the cornea (31), during corpus luteum growth (32), or in aggressive tumor models with active angiogenesis (4). For these reasons, we believe that the skin wounding assay may prove to be a valid and sensitive surrogate angiogenesis assay when effective treatment regimens are used. In fact, a recent report (22) describes reduced vascularization of experimental dermal wounds in patients receiving an antiangiogenic matrix metalloproteinase inhibitor.

The second question raised by this study concerns which assay might be best suited to measure antiangiogenic effects *in situ*. This question is difficult to answer, especially when the mechanism of action of the therapeutic agent is not known. The most commonly used approach to measure "angiogenesis" in tissues is to enumerate microvessel density (*i.e.,* MVD) under the presumption that angiogenic stimulators or inhibitors alter the ratio between blood vessels and other tissue components (*e.g.,* tumor cells). However, tumor growth may be accompanied by proportional blood vessel growth, and conversely, blood vessel regression may be accompanied by a proportional reduction in tumor cells that would not result in a net change in MVD. Therefore, end points other than tumor MVD are clearly required to monitor treatment effect.

Because the mechanism of action of endostatin is not known, we quantified a wide array of vascular parameters to avoid missing subtle effects. All of these measurements have been validated as end points to test the activity of different angiogenesis inhibitors in animal models, but they have not been used in concert. To our knowledge, this is the most comprehensive characterization of blood vessels in an antiangiogenesis study to date. Other investigators have demonstrated that the amount of granulation tissue in murine skin wounds is reduced by overexpression of TSP-1 or by endostatin treatment (28, 33). A number of groups have shown a reduction in vascular density in tissues during administration of angiogenesis inhibitors (3, 34). In one study, the proportional area occupied by blood vessels (similar to the measurement in our study) was reduced in the presence of TSP-1, and this parameter was a more sensitive measure than the reduction in MVD (33).

Angiogenesis inhibitors have been shown to affect endothelial cell kinetics in a number of studies, either by decreasing endothelial cell replication or by inducing apoptosis. The proliferative rate of wound site endothelial cells was diminished by TSP-1 in one experiment (33). Our data indicate a trend toward an endostatin-induced decrease in endothelial cell proliferation in skin wounds, but the difference does not reach statistical significance. Eberhard *et al.* (24) described a wide spectrum of endothelial cell proliferative activity in human tumor samples, which is in keeping with our findings. Several studies have detected induction of endothelial cell apoptosis in tumor blood vessels by antiangiogenic agents (35–37). Interestingly, the pretreatment endothelial cell apoptosis rate in tumor blood vessels was very low (0–2%), which is in striking agreement with our observations in human tumor and wound site vessels.

The assessment of blood vessel maturity by the presence or absence of (smooth muscle-specific actin positive) support cells is well documented (23, 38, 39). Support cell sheathing is thought to stabilize existing blood vessels, whereas the absence of such cells provides a "plasticity window" for vascular remodeling (23, 38). This concept explains why pericyte disengagement occurs before vascular regression. Murine tumors are characterized by a high proportion of immature blood vessels. Benjamin *et al.* (23) observed selective regression of immature blood vessels in murine tumors subjected to vascular endothelial cell growth factor withdrawal, resulting in a dramatic reduction in the percentage of immature vessels.

Lastly, how can the apparent lack of endostatin effect on blood vessels of tumors or wound sites be explained? It is necessary to reinforce the notion that this Phase I trial was not designed to test endostatin efficacy. The apparent lack of endostatin activity should be interpreted with caution for the following reasons: (*a*) The sample size was very small. A total of 21 patients participated in the study, typically with 3 patients per dose level. It should also be noted that ~60% of the tumor biopsy pairs were incomplete because of tumor progression during treatment or lack of sufficient tumor tissue in the sample. (*b*) All patients had end-stage cancer, advanced disease being a study entry requirement. It is possible that endostatin will show effects in earlier stages of tumor development. (*c*) The optimal dose and administration regimen for endostatin and other anti-

angiogenic agents are unknown. (*d*) The assays used in this study to measure antiangiogenic activity may not be optimal.

The endostatin doses used in this study were derived by extrapolation from doses used in animals. Humans may require a higher dose to achieve efficacy. In addition, a single daily infusion had been chosen as the mode of administration for practical reasons. Continuous infusion via i.v. pump may be more advantageous, especially because preliminary pharmacokinetic data indicate that endostatin disappears from the circulation with a half-life of ~12.9 h (40). Interestingly, in mouse experiments, s.c. application of bacterial endostatin-containing inclusion bodies was particularly effective, probably because of slow release of the drug (3).

It is unclear at present what assays would be best suited to measure the antiangiogenic activity of endostatin. This uncertainty is largely attributable to the fact that the mechanism of action of endostatin is unknown. We therefore chose experimental end points (proliferation, apoptosis, and maturation) presumably common to most signaling pathways in endothelial cells. However, the possibility that these measurements are failing to capture a potential antiangiogenic effect cannot be entirely excluded. Nevertheless, tissue-based assays may be useful to optimize antiangiogenic treatment regimens, titrate dosage, and possibly monitor response to angiogenic inhibitors in individual patients.

ACKNOWLEDGMENTS

We are grateful to Toshi Kinoshita for excellent contributions in preparing tissue sections, to Joan Sempf for superb electron microscopy work, and to the residents in Surgical Pathology for processing of the specimens. We also thank Rhoda Arzoomanian for coordinating this trial.

REFERENCES

1. Folkman, J. Fighting cancer by attacking its blood supply. Sci. Am., *275:* 150–154, 1996.

2. Hanahan, D., and Folkman, J. Patterns and emerging mechanisms of the angiogenic switch during tumorigenesis. Cell., *86:* 353–364, 1996.

3. O'Reilly, M. S., Boehm, T., Shing, Y., Fukai, N., Vasios, G., Lane, W. S., Flynn, E., Birkhead, J. R., Olsen, B. R., and Folkman, J. Endostatin: an endogenous inhibitor of angiogenesis and tumor growth. Cell, *88:* 277–285, 1997.

4. Boehm, T., Folkman, J., Browder, T., and O'Reilly, M. S. Antiangiogenic therapy of experimental cancer does not induce acquired drug resistance. Nature (Lond.), *390:* 404–407, 1997.

5. Dhanabal, M., Volk, R., Ramchandran, R., Simons, M., and Sukhatme, V. P. Cloning, expression, and *in vitro* activity of human endostatin. Biochem. Biophys. Res. Commun., *258:* 345–352, 1999.

6. Yamaguchi, N., Anand-Apte, B., Lee, M., Sasaki, T., Fukai, N., Shapiro, R., Que, I., Lowik, C., Timpl, R., and Olsen, B. R. Endostatin inhibits VEGF-induced endothelial cell migration and tumor growth independently of zinc binding. EMBO J., *18:* 4414–4423, 1999.

7. Taddei, L., Chiarugi, P., Brogelli, L., Cirri, P., Magnelli, L., Raugei, G., Ziche, M., Granger, H. J., Chiarugi, V., and Ramponi, G. Inhibitory effect of full-length human endostatin on *in vitro* angiogenesis. Biochem. Biophys. Res. Commun., *263:* 340–345, 1999.

8. Dhanabal, M., Ramchandran, R., Waterman, M. J., Lu, H., Knebelmann, B., Segal, M., and Sukhatme, V. P. Endostatin induces endothelial cell apoptosis. J. Biol. Chem., *274:* 11721–11726, 1999.

9. Dixelius, J., Larsson, H., Sasaki, T., Holmqvist, K., Lu, L., Engstrom, A., Timpl, R., Welsh, M., and Claesson-Welsh, L. Endostatin-induced tyrosine kinase signaling through the Shb adaptor protein regulates endothelial cell apoptosis. Blood, *95:* 3403–3411, 2000.

10. Kim, Y. M., Jang, J. W., Lee, O. H., Yeon, J., Choi, E. Y., Kim, K. W., Lee, S. T., and Kwon, Y. G. Endostatin inhibits endothelial and tumor cellular invasion by blocking the activation and catalytic activity of matrix metalloproteinase. Cancer Res., *60:* 5410–5413, 2000.

11. Shichiri, M., and Hirata, Y. Antiangiogenesis signals by endostatin. FASEB J., *15:* 1044–1053, 2001.

12. Hohenester, E., Sasaki, T., Olsen, B. R., and Timpl, R. Crystal structure of the angiogenesis inhibitor endostatin at 1.5 Å resolution. EMBO J., *17:* 1656–1664, 1998.

13. Sasaki, T., Larsson, H., Tisi, D., Claesson-Welsh, L., Hohenester, E., and Timpl, R. Endostatins derived from collagens XV and XVIII differ in structural and binding properties, tissue distribution and antiangiogenic activity. J. Mol. Biol., *301:* 1179–1190, 2000.

14. Karumanchi, S. A., Jha, V., Ramchandran, R., Karihaloo, A., Tsiokas, L., Chan, B., Dhanabal, M., Hanai, J. I., Venkataraman, G., Shriver, Z., Keiser, N., Kalluri, R., Zeng, H., Mukhopadhyay, D., Chen, R. L., Lander, A. D., Hagihara, K., Yamaguchi, Y., Sasisekharan, R., Cantley, L., and Sukhatme, V. P. Cell surface glypicans are low-affinity endostatin receptors. Mol. Cell, *7:* 811–822, 2001.

15. Chang, Z., Choon, A., and Friedl, A. Endostatin binds to blood vessels in situ independent of heparan sulfate and does not compete for fibroblast growth factor-2 binding. Am. J. Pathol., *155:* 71–76, 1999.

16. Boehm, T., Pirie-Shepherd, S., Trinh, L. B., Shiloach, J., and Folkman, J. Disruption of the KEX1 gene in *Pichia pastoris* allows expression of full-length murine and human endostatin. Yeast, *15:* 563–572, 1999.

17. Dhanabal, M., Ramchandran, R., Volk, R., Stillman, I. E., Lombardo, M., Iruela-Arispe, M. L., Simons, M., and Sukhatme, V. P. Endostatin: yeast production, mutants, and antitumor effect in renal cell carcinoma. Cancer Res., *59:* 189–197, 1999.

18. Kerbel, R. S. Tumor angiogenesis: past, present and the near future. Carcinogenesis (Lond.), *21:* 505–515, 2000.

19. Kerbel, R. S. A cancer therapy resistant to resistance. Nature (Lond.), *390:* 335–336, 1997.

20. Sidky, Y. A., and Auerbach, R. Lymphocyte-induced angiogenesis: a quantitative and sensitive assay of the graft-vs.-host reaction. J. Exp. Med., *141:* 1084–1100, 1975.

21. Hurwitz, H. I., Lockhart, A. C., Dewhirst, M. W., Klitzman, B., Yuan, F., Grichnik, J. N., Proia, A. D., Conway, D. A., Beaty, J. K., Mann, G., and Braun, R. D. Evaluation of wound angiogenesis in healthy volunteers: a potential surrogate marker for antiangiogenesis agents. Proc. Am. Assoc. Cancer Res., *41:* 168, 2000.

22. Lockhart, A. C., Braun, R. D., Dewhirst, M. W., Klitzman, B., Humphrey, J. S., Yuan, F., Grichnik, J. M., Proia, A. D., Conway, D. A., and Hurwitz, H. I. Wound angiogenesis as a potential surrogate marker for anti-angiogenesis clinical trials. Proc. Am. Assoc. Cancer Res., *41:* 168, 2000.

23. Benjamin, L. E., Golijanin, D., Itin, A., Pode, D., and Keshet, E. Selective ablation of immature blood vessels in established human tumors follows vascular endothelial growth factor withdrawal. J. Clin. Investug., *103:* 159–165, 1999.

24. Eberhard, A., Kahlert, S., Goede, V., Hemmerlein, B., Plate, K. H., and Augustin, H. G. Heterogeneity of angiogenesis and blood vessel maturation in human tumors: implications for antiangiogenic tumor therapies. Cancer Res., *60:* 1388–1393, 2000.

25. Dvorak, H. F. Tumors: wounds that do not heal. Similarities between tumor stroma generation and wound healing. N. Engl. J. Med., *315:* 1650–1659, 1986.

26. St. Croix, B., Rago, C., Velculescu, V., Traverso, G., Romans, K. E., Montgomery, E., Lal, A., Riggins, G. J., Lengauer, C., Vogelstein, B., and Kinzler, K. W. Genes expressed in human tumor endothelium. Science (Wash. DC), *289:* 1197–1202, 2000.

27. Berger, A. C., Feldman, A. L., Gnant, M. F., Kruger, E. A., Sim, B. K., Hewitt, S., Figg, W. D., Alexander, H. R., and Libutti, S. K. The

angiogenesis inhibitor, endostatin, does not affect murine cutaneous wound healing. J. Surg. Res., *91:* 26–31, 2000.

28. Bloch, W., Huggel, K., Sasaki, T., Grose, R., Bugnon, P., Addicks, K., Timpl, R., and Werner, S. The angiogenesis inhibitor endostatin impairs blood vessel maturation during wound healing. FASEB J., *14:* 2373–2376, 2000.

29. Klein, S. A., Bond, S. J., Gupta, S. C., Yacoub, O. A., and Anderson, G. L. Angiogenesis inhibitor TNP-470 inhibits murine cutaneous wound healing. J. Surg. Res., *82:* 268–274, 1999.

30. Tanaka, H., Taniguchi, H., Mugitani, T., Koishi, Y., Masuyama, M., Koyama, H., Hoshima, M., and Takahashi, T. Angiogenesis inhibitor TNP-470 prevents implanted liver metastases after partial hepatectomy in an experimental model without impairing wound healing. Br. J. Surg., *83:* 1444–1447, 1996.

31. Brooks, P. C., Clark, R. A., and Cheresh, D. A. Requirement of vascular integrin α v β 3 for angiogenesis. Science (Wash. DC), *264:* 569–571, 1994.

32. Ferrara, N., Chen, H., Davis-Smyth, T., Gerber, H. P., Nguyen, T. N., Peers, D., Chisholm, V., Hillan, K. J., and Schwall, R. H. Vascular endothelial growth factor is essential for corpus luteum angiogenesis. Nat. Med., *4:* 336–340, 1998.

33. Streit, M., Velasco, P., Riccardi, L., Spencer, L., Brown, L. F., Janes, L., Lange-Asschenfeldt, B., Yano, K., Hawighorst, T., Iruela-Arispe, L., and Detmar, M. Thrombospondin-1 suppresses wound healing and granulation tissue formation in the skin of transgenic mice. EMBO J., *19:* 3272–3282, 2000.

34. Blezinger, P., Wang, J., Gondo, M., Quezada, A., Mehrens, D., French, M., Singhal, A., Sullivan, S., Rolland, A., Ralston, R., and Min, W. Systemic inhibition of tumor growth and tumor metastases by intramuscular administration of the endostatin gene. Nat. Biotechnol., *17:* 343–348, 1999.

35. Browder, T., Butterfield, C. E., Kraling, B. M., Shi, B., Marshall, B., O'Reilly, M. S., and Folkman, J. Antiangiogenic scheduling of chemotherapy improves efficacy against experimental drug-resistant cancer. Cancer Res., *60:* 1878–1886, 2000.

36. Bruns, C. J., Harbison, M. T., Davis, D. W., Portera, C. A., Tsan, R., McConkey, D. J., Evans, D. B., Abbruzzese, J. L., Hicklin, D. J., and Radinsky, R. Epidermal growth factor receptor blockade with C225 plus gemcitabine results in regression of human pancreatic carcinoma growing orthotopically in nude mice by antiangiogenic mechanisms. Clin. Cancer Res., *6:* 1936–1948, 2000.

37. O'Reilly, M. S., Holmgren, L., Chen, C., and Folkman, J. Angiostatin induces and sustains dormancy of human primary tumors in mice. Nat. Med., *2:* 689–692, 1996.

38. Benjamin, L. E., Hemo, I., and Keshet, E. A plasticity window for blood vessel remodelling is defined by pericyte coverage of the preformed endothelial network and is regulated by PDGF-B and VEGF. Development, *125:* 1591–1598, 1998.

39. Jain, R. K., Safabakhsh, N., Sckell, A., Chen, Y., Jiang, P., Benjamin, L., Yuan, F., and Keshet, E. Endothelial cell death, angiogenesis, and microvascular function after castration in an androgen-dependent tumor: role of vascular endothelial growth factor. Proc. Natl. Acad. Sci. USA, *95:* 10820–10825, 1998.

40. Thomas, J. P., Schiller, J., Lee, F., Perlman, S., Friedl, A., Winter, T., Marnocha, R., Arzoomanian, R., Alberti, D., Binger, K., Volkman, J., Feierabend, C., Tutsch, K., Dresen, A., Auerbach, R., and Wilding, G. A Phase I pharmacodynamic and pharmacokinetic study of endostatin. Proceedings of the 11th NCI-EORTC-AACR Symposium. 95, 2000.